ACI STRUCTURAL JOURNAL TECHNICAL PAPER

Title no. 95-S31

Analytical Study of Reinforced Concrete Beams Strengthened with Web-Bonded Fiber Reinforced Plastic Plates or Fabrics


by Amir M. Malek, and Hamid Saadatmanesh

Bonding fiber reinforced plastic (FRP) plates or fabrics to the web of reinforced concrete beams can increase the shear and flexural capacity of the beam. This paper presents analytical models to calculate the stresses in the strengthened beam, and the shear force resisted by the composite plate before cracking and after formation of flexural cracks. The anisotropic (orthotropic) behavior of the composite plate or fabric has been considered in the analytical models. The companion paper extends this discussion into post cracking behavior at the ultimate load, where the diagonal shear cracks are formed. The method has been developed assuming perfect bond between FRP and concrete (i.e., no slip), and using compatibility of the strains in the FRP and the concrete beam. The validity of the assumptions used in this method has been verified by comparing the results to the finite element method. A parametric study has been performed to reveal the effect of important variable parameters, such as fiber orientation angle on the shear force resisted by the FRP plate. The method has been developed for both uncracked and cracked beams, and it can be used for stress analysis of these types of beams.

Keywords: analytical; composite; fabric; orthotropic; plated beam; reinforced plastic; repair; retrofit; shear strength; web-bonding.

INTRODUCTION

Many of the nation's constructed facilities are in need of repair, retrofitting, and rehabilitation. Deterioration, aging, and underestimated design loads are the most frequent reasons for strengthening structures. Fiber reinforced plastics (FRP), which have been used in aerospace technology for several decades, are becoming increasingly popular in the construction industry for strengthening purposes. Several attractive properties such as corrosion resistance, ease of fabrication, formability, light weight, and versatility have made FRPs desirable for this construction application. FRPs are made from a variety of fibers and resins.[1] They have been made in different shapes—such as rebars, plates, and fabrics—and have been used in a variety of structural members, including reinforced concrete beams [2-6] and columns,[7-8] and masonry walls.[9]

FRP plates or fabrics have been bonded to the tension face of reinforced concrete beams to increase the bending capacity of the beam. Experimental and theoretical studies on this type of beam have shown a significant increase in the ultimate load and a considerable improvement in cracking behavior. These plates can also be bonded to the web of reinforced concrete beams, as shown in Fig. 1, to increase the shear capacity of the beam.[10] This technique can be used in repair and retrofit of existing beams, as well as in designing new reinforced concrete beams and girders.

Generally, the beams used in the lower floors of multistory buildings resist high shear forces during earthquake. This results in close spacing of the stirrups that may violate spacing requirements given in the codes for proper placing of concrete. By using composite plates or fabrics bonded to the side faces, the designers can increase the spacing of the stirrups.

This paper presents an analytical model to calculate the stresses and the shear force resisted by the composite plate in reinforced concrete beams strengthened with web-bonded FRP plates before cracking, and also after formation of flexural cracks. The companion paper extends this discussion into post cracking behavior at the ultimate load level, where the diagonal shear cracks are formed. The method has been developed based on strain compatibility between the reinforced concrete beam and the FRP plate, and considering the anisotropic behavior of the FRP plate. Equations have been developed for two different cases of uncracked beams, and the beams with flexural cracks. The method has been verified by comparing the it to finite element method. The results of this method also have also been compared to experimental results. A parametric study has been carried out to show the effect of important variable parameters such as the fiber orientation angle, and the geometric properties of the plate on the shear force resisted by the plate.

ACI Structural Journal, V. 95, No. 3, May-June 1998.
Received August 26, 1996, and reviewed under Institute publication policies. Pertinent discussion will be published in the March-April 1999 *ACI Structural Journal* if received by November 1, 1998.

Amir M. Malek received his PhD from the Department of Civil Engineering Mechanics, the University of Arizona, Tucson, where he is now an adjunct faculty member. His current research area is the study of reinforced concrete members strengthened with composite plates or fabrics.

Hamid Saadatmanesh is an associate professor of civil engineering in the Department of Civil Engineering and Engineering Mechanics at the University of Arizona, Tucson. His primary area of research is in the application of advanced composite materials for strengthening and rehabilitation of structures. He is a member and past secretary of ACI Committee 440, Fiber Reinforced Plastic Reinforcement.

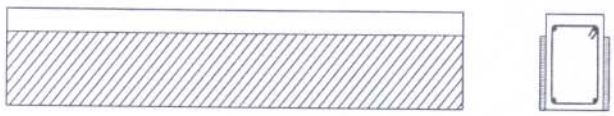

Fig. 1—Shear strengthening of reinforced concrete beams

RESEARCH SIGNIFICANCE

The shear strength of reinforced concrete beams is increased by bonding composite plates to the web of the beam. This paper presents a method to investigate the effect of the plate on the stress distribution in the concrete beam, and also to calculate the shear force carried by the plate. The method has been developed for uncracked beams as well as for beams with flexural cracks. A parametric study has been carried out to reveal the effect of important variable parameters in this strengthening technique. The results of this study can be used to develop design guidelines for concrete beams strengthened for shear with web bonded FRP plates or fabrics.

ANALYTICAL MODEL

The contribution of the FRP plate to the shear capacity of the beam is divided into two parts: Part I, designated by V_p^I, is caused by the anisotropic behavior of the plate and is present even in the regions of pure bending; Part II, designated by V_p^{II}, is caused by the moment gradient in the beam.

In subsequent sections, appropriate equations will be developed to calculate V_p^I and V_p^{II} for both uncracked beams, and beams with flexural cracks. However, first a brief introduction is given into the behavior of orthotropic plates.

The stress-strain relationship in an orthotropic lamina (plate) in any arbitrary system of coordinates such as x-y under plane stress conditions is given by:[11-12]

$$\begin{bmatrix}\sigma_{xx}\\ \sigma_{yy}\\ \sigma_{xy}\end{bmatrix} = \begin{bmatrix}\overline{Q_{11}}\,\overline{Q_{12}}\,\overline{Q_{13}}\\ \overline{Q_{12}}\,\overline{Q_{22}}\,\overline{Q_{23}}\\ \overline{Q_{13}}\,\overline{Q_{23}}\,\overline{Q_{33}}\end{bmatrix}\begin{bmatrix}\varepsilon_{xx}\\ \varepsilon_{yy}\\ \gamma_{xy}\end{bmatrix} \quad (1)$$

where $[\overline{Q}]$ represents the transformed stiffness matrix of the lamina, and its elements are:

$$\begin{aligned}
\overline{Q_{11}} &= Q_{11}C_0^4 + 2(Q_{12}+2Q_{33})S_0^2C_0^2 + Q_{22}S_0^4\\
\overline{Q_{12}} &= Q_{12}(S_0^4+C_0^4) + (Q_{11}+Q_{22}-4Q_{33})S_0^2C_0^2\\
\overline{Q_{22}} &= Q_{11}S_0^4 + 2(Q_{12}+2Q_{33})S_0^2C_0^2 + Q_{22}C_0^4\\
\overline{Q_{13}} &= (Q_{11}-Q_{12}-2Q_{33})S_0C_0^3 + (Q_{12}-Q_{22}+2Q_{33})S_0^3C_0\\
\overline{Q_{23}} &= (Q_{11}-Q_{12}-2Q_{33})S_0^3C_0 + (Q_{12}-Q_{22}+2Q_{33})S_0C_0^3\\
\overline{Q_{33}} &= (Q_{11}+Q_{22}-2Q_{12}-2Q_{33})S_0^2C_0^2 + Q_{33}(S_0^4+C_0^4)
\end{aligned} \quad (2)$$

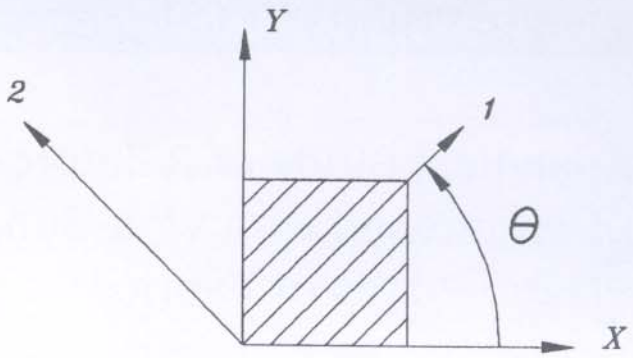

Fig. 2—Definition of fiber orientation angle

In the above expressions, $S_0 = \sin\theta$ and $C_0 = \cos\theta$, where θ is the angle between the x axis and the longitudinal axis (fiber direction) of the FRP plate, measured counter-clockwise as shown in Fig. 2. Furthermore:

$$\begin{aligned}
Q_{11} &= \frac{E_{11}}{1-\nu_{12}\nu_{21}}\\
Q_{22} &= \frac{E_{22}}{1-\nu_{12}\nu_{21}}\\
Q_{12} &= \nu_{21}\frac{E_{11}}{1-\nu_{12}\nu_{21}}\\
Q_{33} &= G_{12}
\end{aligned} \quad (3)$$

where 1 and 2 refer to the longitudinal (fiber) and transverse directions in the composite plate, respectively, as shown in Fig. 2. Therefore, E_{11} and E_{22} are the elastic moduli of the plate in the longitudinal and transverse directions, G_{12} is the shear modules of the plate, and ν is the Poisson's ratio.

In order to show the effect of the plate on the stress distribution in the reinforced concrete beam strengthened with web-bonded FRP plates, two cases are considered: (a) uncracked beam; and (b) cracked beam.

I—Uncracked beam

The following assumptions are made in developing this method:

- Plane sections remain plane.
- Complete composite action between the FRP plate and concrete beam (i.e., no slip).
- Linear elastic materials.

Shear due to anisotropic (orthotropic) behavior of FRP plate under pure bending, V_p^I

In pure bending:

$$\begin{aligned}
\sigma_{yy} &= 0\\
\gamma_{xy} &= 0
\end{aligned} \quad (4)$$

where x is the longitudinal axis of the beam, and y is perpendicular to the x in the plane of the beam. Therefore, σ_{yy} and γ_{xy} are transverse normal stress and shear strain, respectively.

The validity of these assumptions will be verified by the finite element analysis in subsequent sections.

Expanding the second row of Eq. (1) to find σ_{yy} results in:

$$\sigma_{yy} = \overline{Q_{12}}\varepsilon_{xx} + \overline{Q_{22}}\varepsilon_{yy} + \overline{Q_{23}}\gamma_{xy} \tag{5}$$

This stress as well as γ_{xy} are negligible and according to Eq. (4) can be assumed as zero; therefore, ε_{yy} is written as:

$$\varepsilon_{yy} = -\frac{\overline{Q_{12}}}{\overline{Q_{22}}}\varepsilon_{xx} \tag{6}$$

Replacing ε_{yy} from Eq. (6) and γ_{xy} from Eq. (4) in to the first and the third rows of Eq. (1), the normal and shear stresses in the FRP plate are written as:

$$\sigma_{xx} = Qs_{11}\varepsilon_{xx} \tag{7}$$

$$\tau_{xy} = Qs_{13}\varepsilon_{xx} \tag{8}$$

where Qs_{11} and Qs_{13} are given by:

$$Qs_{11} = \overline{Q_{11}} - \frac{\overline{Q_{12}}^2}{\overline{Q_{22}}} \tag{9}$$

$$Qs_{13} = \overline{Q_{13}} - \frac{\overline{Q_{23}}\,\overline{Q_{12}}}{\overline{Q_{22}}} \tag{10}$$

The cross section of the strengthened beam as well as the assumed linear strain variations across the depth of the cross section of the beam are shown in Fig. 3. The strains in the steel rebars located in the tension and compression zones ε_s and ε_s', the strain at the top of the FRP plate ε_p, and the maximum tensile strain in the concrete beam ε_t are related to the maximum compressive strain in the concrete ε_c through the following expressions:

$$\begin{aligned}
\varepsilon_s &= \varepsilon_c\frac{d-\bar{y}}{\bar{y}}\\
\acute{\varepsilon}_s &= \varepsilon_c\frac{\bar{y}-\acute{d}}{\bar{y}}\\
\varepsilon_p &= \varepsilon_c\frac{\bar{y}-d_p}{\bar{y}}\\
\varepsilon_t &= \varepsilon_c\frac{h-\bar{y}}{\bar{y}}
\end{aligned} \tag{11}$$

These strains as well as $\bar{y}$ (location of the neutral axis) are shown in Fig. 3. Based these strains, and using the stress-strain relationship of each material, the stresses and forces acting on the cross section of the strengthened beam are calculated. The stress and the force in the steel rebars are calculated by multiplying the strain by the modulus of elasticity and the area of the rebars, respectively. The strain at any point of the concrete and FRP plate is related to the maximum concrete compressive strain ε_c based on a linear strain variation across the depth of the cross section as shown in Fig. 3. The stress in the FRP along the axis of the beam is calculated using Eq. (7), relating the strain in the plate to its corresponding stress. The force in the FRP plate is then calculated by integrating the stress over the cross-sectional

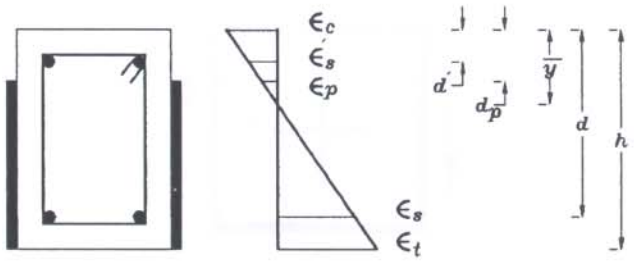

Fig. 3—Strain variation in the strengthened beam

area of the plate. The stress and the force in the concrete are calculated assuming linear elastic behavior by multiplying the strain by the concrete modulus of elasticity and then integrating over the cross section of the beam. The location of the neutral axis $\bar{y}$ is obtained by solving the equation of equilibrium of horizontal forces across the depth of the cross section:

$$\bar{y} = \frac{Qs_{11}t_pd_p^2 - E_cbh^2 - 2A_sE_sd - 2\acute{A}_sE_s\acute{d} - Qs_{11}t_ph^2}{2(d_pt_pQs_{11} - E_cbh - E_sA_s - E_s\acute{A}_s - Qs_{11}t_ph)} \tag{12}$$

where

t_p = sum of the thicknesses of the plates on both faces of the beam
E_c = elastic modules of concrete
b = width of concrete beam
A_s = area of reinforcement in tension zone of concrete
$\acute{A}_s$ = area of steel reinforcement in the compression zone of concrete.

The compressive strain in concretes ε_c is calculated from:

$$\varepsilon_c = \frac{M}{S^*} \tag{13}$$

where M is the moment of all internal forces about the neutral axis, and S^* is defined as:

$$\begin{aligned}
S^* = {} & \bar{y}[-Qs_{11}t_p(d_p-h) + E_sA_s + E_s\acute{A}_s + E_cbh] + \\
& Qs_{11}t_p(d_p^2-h^2) - 2dE_sA_s - 2\acute{d}E_s\acute{A}_s - h^2bE_c + \\
& \left[\frac{1}{3}Qs_{11}t_p(h^3-d_p^3) + E_sA_sd^2 + \frac{1}{3}E_cbh^3 + E_s\acute{A}_s\acute{d}^2\right]\frac{1}{\bar{y}}
\end{aligned} \tag{14}$$

Knowing $\bar{y}$ and ε_c, the normal strain at any point on the plate is calculated from:

$$\varepsilon_{xx} = -\frac{y}{\bar{y}}\varepsilon_c \tag{15}$$

where y is the distance from the neutral axis of the strengthened beam (positive if the point is above the neutral axis).

Using Eq. (8) the shear stress at any point of the plate is obtained:

$$\tau_{xy} = -Qs_{13}\frac{y}{\bar{y}}\varepsilon_c \tag{16}$$

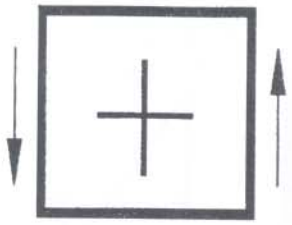

Fig. 4—Conventional positive sign for V_p^I

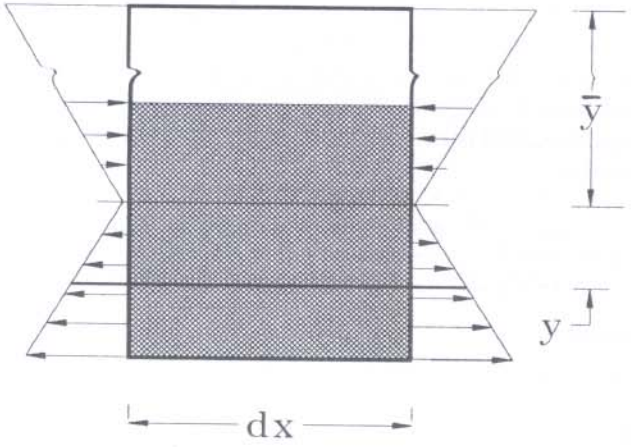

Fig. 5—Stresses acting on an infinitesimal part of the beam

The shear force in the FRP plate is calculated by integrating the above shear stress over the cross section of the plate, and is given by the following equation:

$$V_p^I = -\frac{\varepsilon_c Q s_{13} t_p}{2\bar{y}}(d_p^2 - h^2 + 2\bar{y}h - 2\bar{y}d_p) \qquad (17)$$

The superscript *I* is used to indicate the portion "*I*" of the total shear that is present even under pure bending. The conventional positive sign of this force is shown in Fig. 4.

Shear due to moment gradient V_p^{II}

Generally, each section of the beam undergoes bending moment and shear force at the same time. To find the portion of the shear force in the FRP plate, which is caused by the variation of the bending moment in the beam (shear force), an infinitesimal section of the strengthened beam *dx*. as shown in Fig. 5, is considered. The same procedure as that for V_p^I is followed to find ε_c and the corresponding stresses across the depth of the section. The free-body diagram for an isolated part of the plate between the bottom face and a section at distance y from the neutral axis is shown in Fig. 6. The increment of the force *dF* is calculated from:

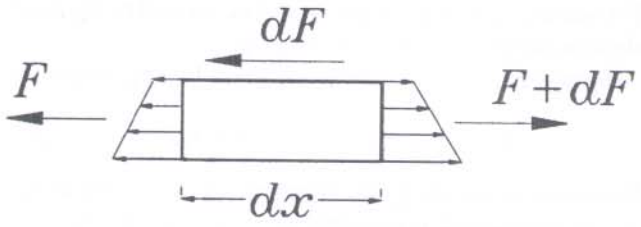

Fig. 6—Free body diagram of a small part of the plate

$$dF = \int_{-(h-\bar{y})}^{y} (d\sigma_{xx} t_p) dy \qquad (18)$$

where

$$d\sigma_{xx} = Q s_{11}\left(-\frac{y}{\bar{y}}\right)\frac{dM}{S^*} \qquad (19)$$

The horizontal shear stress acting on the plate at distance *y* from the neutral axis is calculated by dividing *dF* by the area of the plate:

$$\tau = \frac{dF}{t_p dx} \qquad (20)$$

Substituting Eq. (19) in Eq. (18), performing the integration to find *dF*, and then substituting *dF* into Eq. (20), the shear stress in the plate at any point located at distance *y* from the neutral axis is obtained from:

$$\tau = \frac{Q s_{11} V}{2\bar{y}S^*}[-y^2 + (h-\bar{y})^2] \qquad (21)$$

The total shear force acting on the section of the plate due to moment gradient is then calculated from:

$$V_p^{II} = \int_{-(h-\bar{y})}^{\bar{y}-d_p} \tau t_p dy \qquad (22)$$

Superscript *II* indicates that this component of the shear force is due to the increment in the bending moment. Substituting the shear stress given in Eq. (21) in the above equation and integrating, the shear force is obtained:

$$V_p^{II} = \frac{Q s_{11} t_p V}{2\bar{y}S^*}\left(\frac{2h^3}{3} + \frac{d_p^3}{3} - \bar{y}h^2 - d_p h^2 - \bar{y}d_p^2 + 2d_p\bar{y}h\right) \qquad (23)$$

The conventional positive sign for the above shear force is shown in Fig. 7. This convention is selected for consistency of signs in beam theory and signs assumed for developing the stress-strain relationship in the anisotropic FRP plate. The total shear force in the plate V_p is the algebraic sum of the forces given by Eq. (17) and (23):

$$V_p = -V_p^I + V_p^{II} \qquad (24)$$

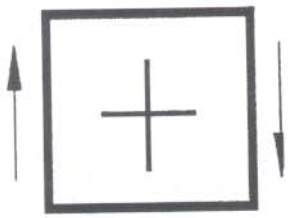

Fig. 7—Conventional positive sign for V_p^{II}

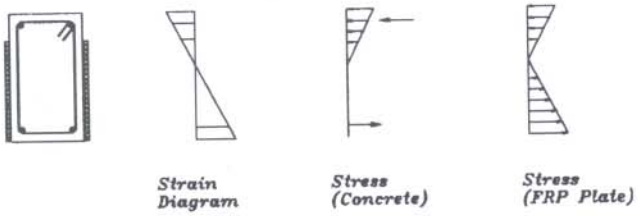

Fig. 8—Strain and stress diagrams in the strengthened cracked beam

It is noted that generally the numerical value of V_p^I will be negative according to the above assumed sign convention, resulting in addition of V_p^I and V_p^{II}. The shear force resisted by the reinforced concrete beam alone is given by:

$$V_c = V - V_p \tag{25}$$

where

V = shear force due to external loads

II—Beam with flexural cracks

The procedure explained for uncracked beam can be followed for strengthened cracked beam. It is assumed that concrete does not resist any tensile stress after cracking. The strain and stress diagrams of a typical section of the strengthened beam under pure bending are as shown in Fig. 8. Using a procedure similar to uncracked beam, and writing the equilibrium equation of the horizontal forces acting on the cross section of the beam, the following equation for the distance to the neutral axis from the top concrete fiber in compression $\bar{y}$ is obtained:

$$A\bar{y}^2 + B\bar{y} + C = 0 \tag{26}$$

where

$$\begin{aligned} A &= -\frac{1}{2}E_c b + \frac{1}{2}t_p Q s_{11} \\ B &= -E_s \acute{A}_s - E_s A_s - h t_p Q s_{11} \\ C &= E_s \acute{A}_s \acute{d} + E_s A_s d + \frac{1}{2}h^2 t_p Q s_{11} \end{aligned} \tag{27}$$

The parameters used in the above equations were defined previously. Similar to the uncracked beam, the maximum compressive strain at the top of the section ε_c is obtained by writing the moment equilibrium equation of the section as:

$$\varepsilon_c = \frac{M}{S_c^*} \tag{28}$$

where

$$S_c^* = \frac{1}{3}E_c b\bar{y}^2 + \frac{1}{\bar{y}}\left[E_s \acute{A}_s(\bar{y} - \acute{d})^2 + E_s A_s(d - \bar{y})^2 + \frac{1}{3}Q s_{11} t_p (h - \bar{y})^3\right] \tag{29}$$

Again, using the procedure for the uncracked beam, V_p^I, which is the shear force in the plate due to pure bending of the beam, is obtained from:

$$V_p^I = \frac{t_p}{2\bar{y}} Q s_{13} \varepsilon_c (h - \bar{y})^2 \tag{30}$$

For this case, V_p^{II} is not different from the uncracked beam and Eq. (23) is still valid.

The validity of the basic assumptions used in developing this method has been verified by comparing its results to the finite element method. The method has also been used in a parametric study to investigate the effects of important variable parameters such as the fiber orientation angle, and the thickness of the plate on the shear force carried by the concrete beam.

CASE STUDY

In order to demonstrate the application of this method, and also to verify the validity of the assumptions used in this study, a reinforced concrete beam strengthened with FRP plates bonded to the web was studied. The geometry of this beam and the location of the plates are shown in Fig. 9. The mechanical properties of the materials are given in Table 1. Furthermore, the shear modules of the composite plate G_{12} was assumed as 6.3 GPa (914 ksi).

Using Eq. (3), the elements of the stiffness matrix of the plate are obtained:

Q_{11} = 34,664 GPa (5,026,280 ksi)
Q_{12} = 1484 GPa (215,180 ksi)
Q_{22} = 4124 GPa (597,980 ksi)
Q_{33} = 6300 GPa (913,500 ksi)

Verification of the method

The finite element method was used to verify the validity of the assumptions used in developing the analytical model. The computer program ABAQUS version 5.4 was used for this purpose. Considering the lack of the external lateral forces, a two-dimensional analysis (plane stress) was used for this study. A mesh of four-node elements was used to model the concrete beam. Rebars were modeled as one-dimensional bar elements. Four-node composite membrane elements were used to model the FRP plate.[13] The same nodes that were used for concrete elements were

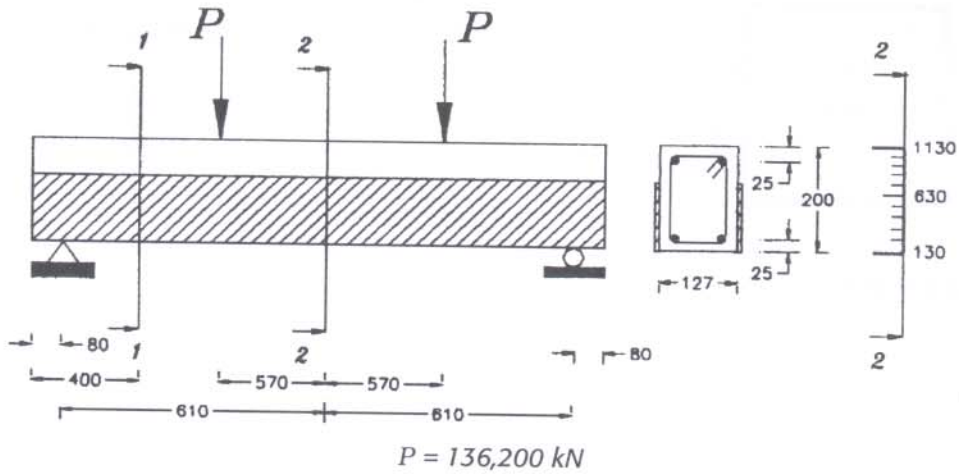

Fig. 9—Geometry of the strengthened beam, and node definition along section 2

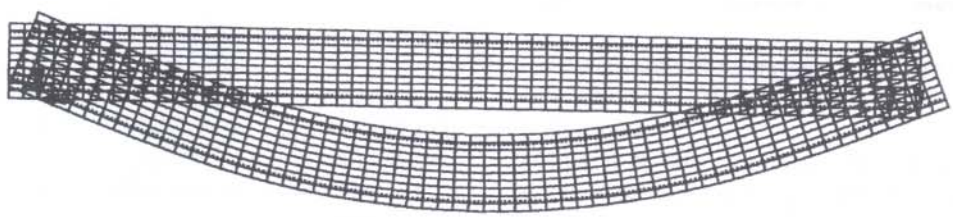

Fig. 10—Mesh definition and deflection of the beam

also used to define the membrane elements. In this manner the stiffness of the membrane elements was added to the stiffness of the concrete elements appropriately. The mesh definition and the deflected shape of the beam under the applied loads are shown in Fig. 10.

Fiber orientation was assumed as 45 deg and the variation of

$$\left|\frac{\varepsilon_{xy}}{\varepsilon_{xx}}\right| \text{ and } \left|\frac{\sigma_{yy}}{\sigma_{xx}}\right|$$

along Section 2 shown in Fig. 9 were studied. The node numbering along this section of the beam is also shown in Fig. 9. The finite element results are listed in Table 2.

As can be seen from the results in this table, both ratios are negligibly small confirming the assumption made in Eq. (4). The variation of the maximum compressive strain in the concrete along the beam has also been compared to the finite element results in Fig. 11. This figure shows a close agreement between the results of this method and the results of finite element analysis.

Comparison to experimental results

The results predicted by this method were compared to the test results of two precracked flexural specimens IA and IIA in an experimental study by Norris et al.[10] The geometry of these beams is shown in Fig. 9. The ultimate loads of these beams were reported as P = 68.97 kN (15.5 kips) and 62.29 kN (14 kips), respectively. The fiber orientation angle for both beams was zero deg, and the thicknesses of the composite fabric were 0.33 mm (0.013 in.), and 0.66 mm (.026 in.), respectively. The mechanical properties of the composite fabric used in Beam IA are those given in Table 1, and for Beam IIA were slightly different.[10] At the ultimate load, the axial strain in the composite plate at the center of the beam was calculated as 0.00781 and 0.00608 in Beams IA and IIA, respectively. The corresponding measured results were 0.0072 and 0.0056, respectively. This shows a reasonably close agreement between the experimental and theoretical

Table 1—Mechanical properties of the materials

Material	Elastic modules, GPa (ksi)	Poisson's ratio
Concrete	27.9 (4046)	0.18
Steel	200 (29,000)	0.3
FRP	E_{11} = 34.13 (4949) E_{22} = 4.06 (589)	ν_{12} = 0.36

Table 2—Variation of $\left|\frac{\varepsilon_{xy}}{\varepsilon_{xx}}\right|$ and $\left|\frac{\sigma_{yy}}{\sigma_{xx}}\right|$ along Section 2

Node numbers	$\left\|\frac{\varepsilon_{xy}}{\varepsilon_{xx}}\right\|$	$\left\|\frac{\sigma_{yy}}{\sigma_{xx}}\right\|$
130	0.063	0.058
230	0.079	0.037
330	0.059	0.039
430	0.071	0.043
530	0.070	0.050
730	0.070	0.028
830	0.070	0.034
930	0.059	0.036
1030	0.079	0.036
1130	0.063	0.058

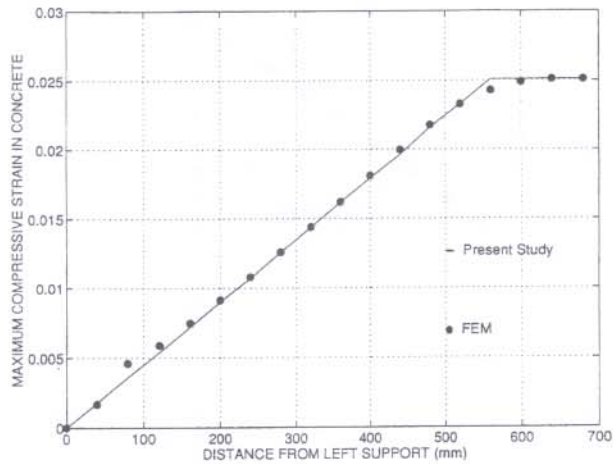

Fig. 11—Comparison of the present method to FEM

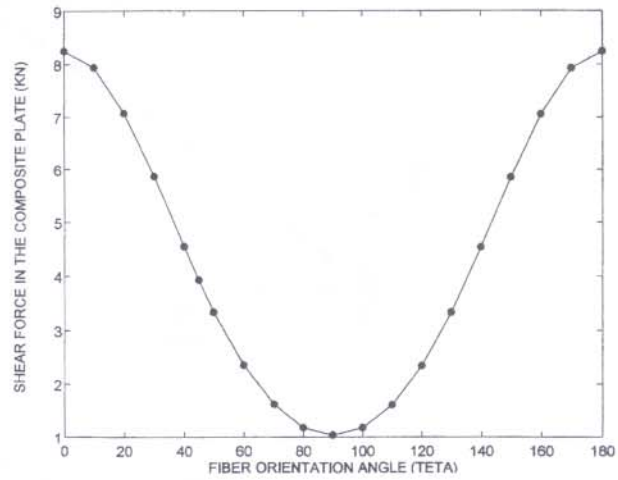

Fig. 12—Variation of the shear force resisted by the plate against fiber orientation angle (uncracked beam)

results. The difference is mainly due to the simplifying assumptions made in analysis, such as ignoring slip and assuming linear elastic assumption.

Parametric study

The effect of important parameters such as the fiber orientation angle was investigated through a parametric study. This study was carried out for both uncracked and cracked beams, and the variation of the resisting shear force developed in the composite fabric was the focus of this parametric study.

I—Uncracked beam

The effect of the fiber orientation angle was studied for Section 1 shown in Fig. 9. At this section of the beam, the shear force and bending moment are $V = 136.2$ kN (30.62 kips); and $M = 54.48$ kN-m (48.2 kip-in.), respectively. It is assumed that the composite plate has a uniform thickness of 4 mm (0.16 in.) and that it covers the entire depth of the concrete beam, that is $d_p = 0$. The variation of the shear force resisted by the plate V_p vs. fiber orientation angle is shown in Fig. 12. As can be seen from this figure, the maximum shear force in the plate is only about 6 percent of the shear force acting on the section of the strengthened beam. This force is mainly caused by the internal shear force V_p^{II} and its maximum value occurs when $\theta = 0$. This indicates that the effect of the plate is relatively insignificant before cracking.

The beam was also studied with four different fiber orientation angles of 0, 45, 90, and 135 deg and different plate thicknesses. The variation of the shear force in the fabric vs. fabric thickness is shown in Fig. 13. As can be seen from this figure, the contribution of the plate to the shear capacity of the beam increases almost linearly with the increase in the plate thickness.

The third part of this parametric study was concentrated on the effect of the plate height on the shear force in the composite plate. The thickness of the plate was assumed 4 mm, and two different fiber orientations of 45 and 135 deg were studied. The effect of d_p, which is inversely proportional to the height of the composite plate, was investigated. The variation of V_p vs. d_p is shown in Fig. 14. As shown in this figure, for both fiber orientations the maximum shear force occurs when the plate stops at a point near the neutral axis of the strengthened beam. The significance of the fiber orientation angle on the shear force resisted by the plate is also shown in this figure.

II—Beam with flexural cracks

The geometry of the beam was assumed the same as the uncracked beam. It was assumed that due to a high bending moment in the section there were flexural cracks in the reinforced concrete beam. The variation of the shear force vs. the fiber orientation angle, as well as the thickness of the plate are shown in Fig. 15 and 16, respectively. In this case, the concrete in the tension zone does not resist any tensile stress since it is assumed to have cracked, which results in higher tensile stresses in the fabric as well as the steel rebars. Both normal and shear stress in the fabric are proportional to the maximum strain in the concrete. Therefore, the shear stress, and consequently the shear force in the composite fabric are considerably higher in cracked beams than in uncracked beams. Furthermore, due to cracking, the relationship between the thickness of the fabric and the contribution of the fabric to the shear resistance of the beam is no longer linear. The maximum effect of the fabric occurs where the fiber orientation angle is about 135 deg. At this angle the two components used in calculating V_p are added, resulting in the highest effect of the fabric.

SUMMARY AND CONCLUSIONS

The effect of the composite fabric or plate bonded to the web of reinforced concrete beams on the shear force carried by the concrete beam was investigated. Closed form solutions were developed based on the compatibility of the strains in the plate and the beam, assuming that the materials behaved linearly elastic, and that there was complete composite action between the fabric and the beam (i.e., no slip). The shear force in the fabric is assumed composed of two different components. The first one is caused by the orthotropic behavior of the fabric. This component is present even if the beam resists only pure bending. The second component, which is caused

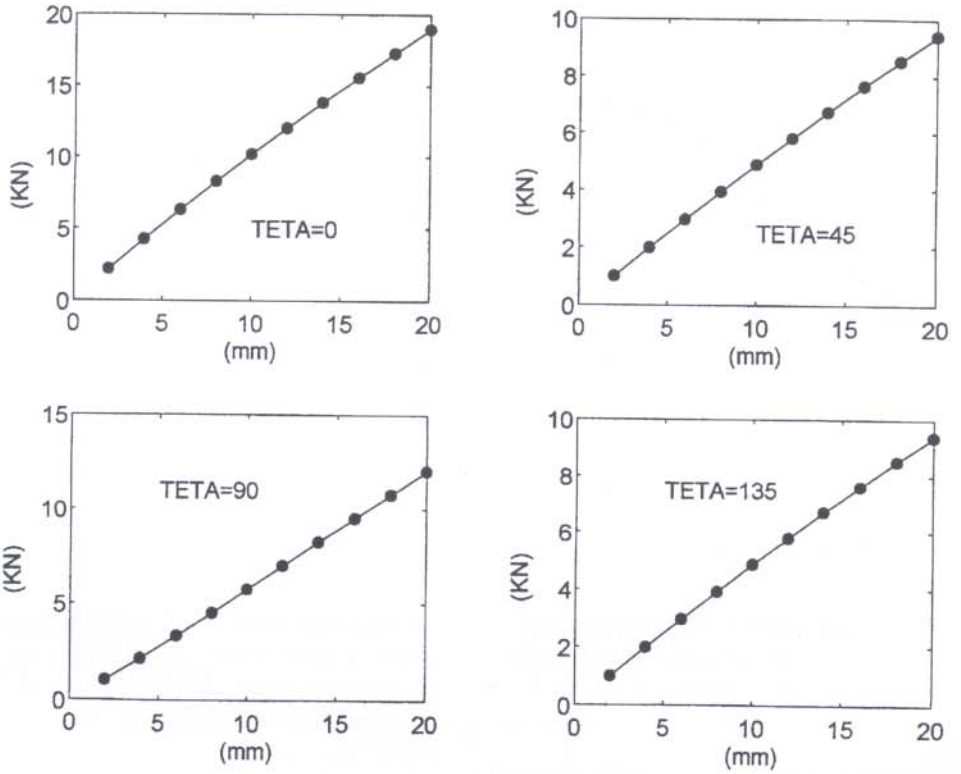

Fig. 13—Variation of the shear force resisted by the plate (N) against thickness of the plate (mm) for different fiber orientation angles (uncracked beam)

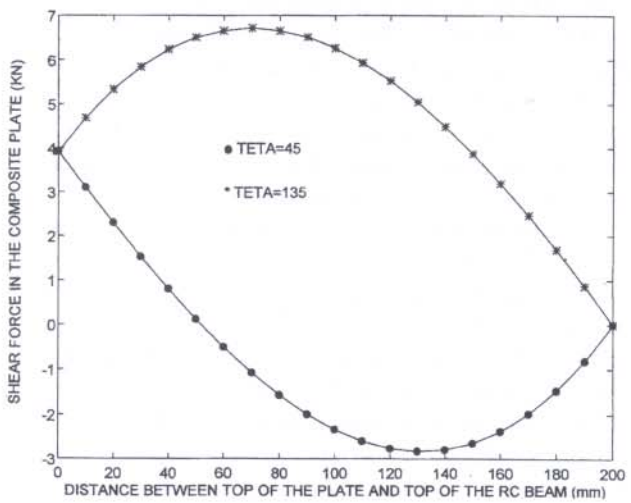

Fig. 14—Variation of the shear force resisted by the plate against height of the plate (uncracked beam)

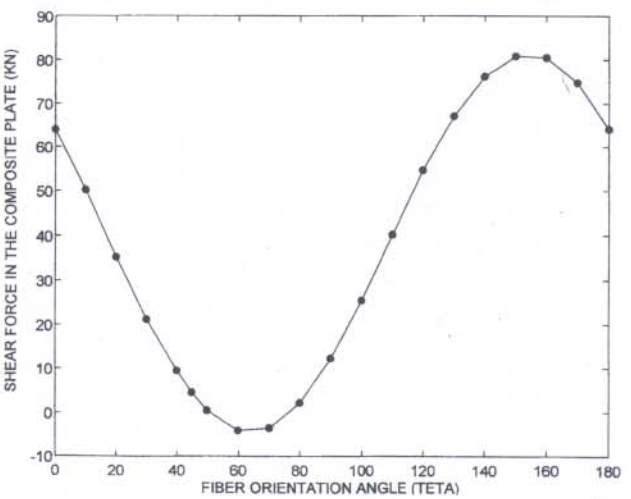

Fig. 15—Variation of the shear force in the plate against fiber orientation angle (cracked beam)

by the variations of the bending moment (internal shear force on the section), is calculated in a manner similar to that of isotropic plate or fabric. Two different cases of uncracked and flexurally cracked beams were studied. It was concluded that for the uncracked beam, the shear force resisted by the composite fabric was negligible. However, for beam with flexural cracks, this force was considerably higher, and depended on the thickness and the fiber orientation of the fabric or plate. In general, the maximum tensile stress in a strengthened reinforced concrete beam can be calculated by using the method described here, and assuming that the concrete is uncracked. This stress can then be compared to the modules of rupture of concrete, to investiate if the concrete beam is cracked. Using the appropriate equations presented in this paper, the maximum compressive strain in concrete, stresses acting at different points of the section, and the shear force in the concrete beam are calculated. The following summarizes the steps involved in the calculation of stresses and strains in the FRP fabric or plate as well as the shear force resisted by the fabric:

1. Obtain the depth of neutral axis $\bar{y}$ using Eq. (12) (Eq. [26] for cracked section).

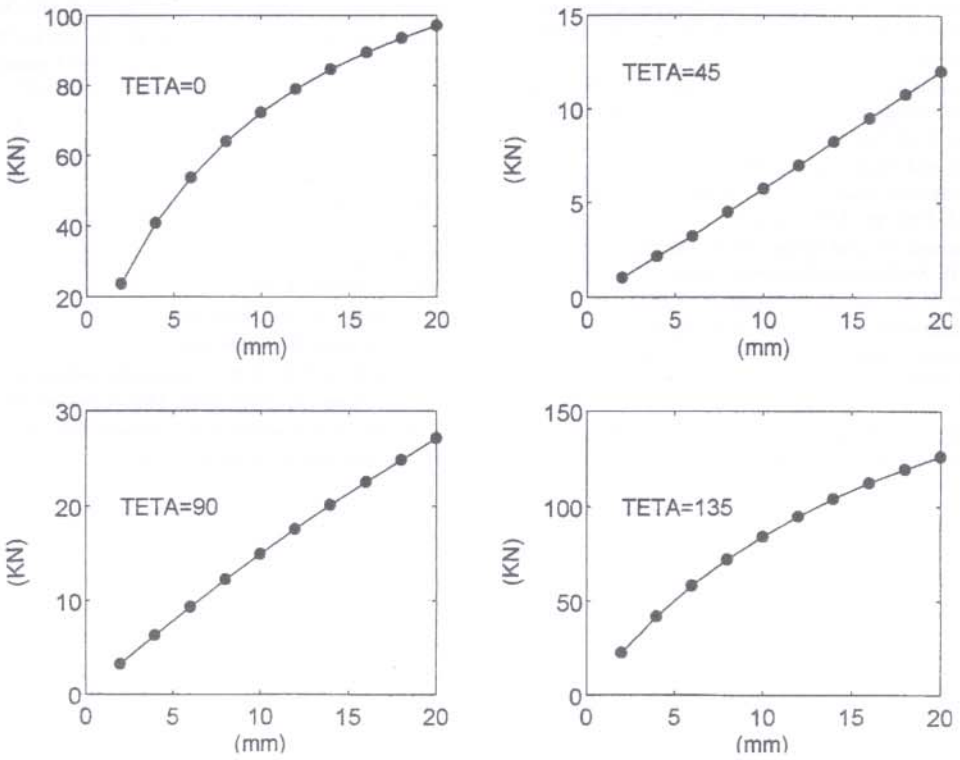

Fig. 16—Variation of the shear force in the plate (N) against thickness of the plate (mm) for different fiber orientation angles (cracked beam)

2. Calculate the maximum compressive strain in the concrete using Eq. (13) (Eq.[28] for cracked section) gives the maximum compressive strain the concrete.

3. Calculate the axial strain in the composite plate using Eq. (15).

4. Calculate the stresses in the composite plate or fabric using Eq. (7) or (8).

5. Determine the stress in the composite plate in the desired direction using the classical stress transformation equations.

6. Finally, calculate the resisting shear force of the plate V_p from Eq. (24) using appropriate terms for cracked or uncracked sections.

ACKNOWLEDGEMENTS

The research reported in this paper was sponsored by the NAtional Science Foundation (NSF) through grant no. 9257344. The support from NSF is greatly appreciated. The findings and opinions presented in this paper are those of the authors and do not reflect the views of the National Science Foundation.

NOTATION

A = coefficient used in defining depth of the neutral axis
A_s = area of the steel reinforcement in the tension zone of concrete
A_s = area of the steel reinforcement in the compression zone of concrete
B = coefficient used in defining depth of the neutral axis
b = width of the concrete beam
C = coefficient used in defining depth of the neutral axis
C_o = parameter related to the fiber orientation angle
d = depth of the longitudinal tensile reinforcement
d_p = distance between top of the plate and top of the concrete beam
d = depth of the longitudinal compressive steel reinforcement
E_c = elastic modules of the concrete
E_{11} = longitudinal elastic modules of the FRP plate
E_{22} = transverse elastic modules of the FRP plate
F = axial force acting on a part of composite plate
G_{12} = shear modules of the composite plate
h = height of the concrete beam
M = internal bending moment
Q = coefficient used in definition of transverse stiffness matrix
$\bar{Q}$ = elements of the transformed stiffness matrix
S^* = parameter used in calculation of the maximum compressive strain in concrete
S_c^* = parameter used in calculation of the maximum compressive strain in concrete
S_o = coefficient used in definition of transformed stiffness matrix
t_p = total thickness of the composite plate on the side faces of the concrete beam
V = internal shear force
V_p^I = first component of the shear force resisted by the plate
V_p^{II} = second component of the shear force resisted by the plate
y = distance from neutral axis
y = depth of the neutral axis
σ_{xx} = normal stress in x direction
σ_{yy} = normal stress in y direction
σ_{xy} = shear stress
θ = fiber orientation angle
ν = Poisson's ratio
ε_c = maximum compressive strain in concrete
ε_s = axial strain in longitudinal steel reinforcement in tension zone
ε_s = axial strain in longitudinal steel reinforcement in compression zone
ε_t = maximum tensile strain in concrete
ε_{xx} = axial strain in x direction
ε_{yy} = axial strain in y direction
ε_{xy} = shear strain
τ = shear stress

REFERENCES

1. Malek, A. M., and Saadatmanesh, H., "Physical and Mechanical Properties of Typical Fibers and Resins," *Proceedings*, First International Conference on Composites in Infrastructure, Tucson, Ariz., Jan. 15-17, 1996, pp. 68-79

2. Swamy, R. N.; Jones, R.; and Bloxham, J. W., "Structural Behavior of Reinforced Concrete Beams Strengthened by Epoxy-Bonded Steel Plates," *The Structural Engineer*, V. 65A, No. 2, Feb. 1987, pp. 59-68.

3. Ritchie, P. A.; Thomas, D. A.; Lu, L.-W.; and Connelly, G. M., "External Reinforcement of Concrete Beams Using Fiber Reinforced Plastics," *ACI Structural Journal*, V. 88, No. 4, 1991, pp. 490-500.

4. Saadatmanesh, H., and Ehsani, M. R., "RC Beams Strengthened with GFRP Plates I: Experimental Study," *ASCE Journal of Structural Engineering*, V. 117, No. 11, 1991, pp. 3417-3433.

5. An, W.; Saadatmanesh, H.; and Ehsani, M. R., "RC Beams Strengthened with FRP Plates II: Analysis and Parametric Study," *ASCE Journal of Structural Engineering*, V. 117, No. 11, 1991, pp. 3434-3455.

6. Malek, A. M.; Saadatmanesh, H.; and Ehsani, M. R., "Prediction of Failure Load of RC Beams Strengthened with FRP Plate due to Stress Concentration at the Plate End," *ACI Structural Journal*, V. 95, No. 2, Mar.-Apr. 1998, pp. 142-152.

7. Saadatmanesh, H; Ehsani, M. R.; and Li, M. W. "Strength and Ductility of Concrete Columns Externally Reinforced with Fiber Composite Straps," *ACI Structural Journal*, V. 91, No. 4, July-Aug. 1994, pp. 434-447.

8. Saadatmanesh, H; Ehsani, M. R.; and Jin, L., "Seismic Strengthening of Circular Bridge Pier Models with Fiber Composites," ACI Structural Journal, V. 93, No. 6, Nov.-Dec. 1996, pp. 639-647.

9. Ehsani, M. R., and Saadatmanesh, H., "Out-of-plane Strength of Masonry Walls Retrofitted with Fiber Composites," *Proceedings*, Workshop on Seismic Behavior of Infilled Frames, National Center of Earthquake Engineering Research, San Francisco, Calif., 1994.

10. Norris, T.; Saadatmanesh, H.; and Ehsani, M. R., "Shear and Flexural Strengthening of RC Beams with Carbon Fiber Sheets," *ASCE Journal of Structural Engineering*, V. 123, No. 7, July 1997, pp. 903-911.

11. Jones, R. M., *Mechanics of Composite Materials*, McGraw-Hill Book Company, New York, 1975.

12. Mallick, P. K., *Fiber reinforced Composites, Materials Manufacturing and Design*, Second Edition, Marcel Dekker, Inc., 1993.

13. *ABAQUS/Standard User's Manual*, Vols. I and II, Version 5.4, Hibbitt Karlsson and Sorensen Inc., 1994.

Authorized reprint from: May-June 1998 issue of ACI Structural Journal